

Lepton Polarization asymmetries in $B \rightarrow X_s \tau^+ \tau^-$ in MSSM

Naveen Gaur*

Department of Physics & Astrophysics, University of Delhi, Delhi - 110 007, India

(Dated: May 26, 2020)

Semi-leptonic and leptonic decays of B-mesons are important probes for testing SM and theories beyond it because of their relative cleanliness and far less theoretical uncertainties. In semi-leptonic decays based on quark level transition $b \rightarrow s \ell^+ \ell^-$ apart from branching ratio one can study many other (possible) observables associated with final state leptons like, lepton pair Forward Backward asymmetry, lepton polarization asymmetries etc. But as proposed recently if we can tag the B-meson than one can measure the polarization asymmetries of both the leptons. Here we will study the polarization asymmetries of both the final state leptons in SM and Minimal Supersymmetric Extension (MSSM) to it

PACS numbers:

I. INTRODUCTION

The rare B-meson decays induced by Flavor Changing Neutral Current (FCNC) $b \rightarrow s(d)$ transitions arises only at loop levels in Standard Model (SM). Because these transitions occur at loop level, hence provides useful tests of the detailed structure of the theory at the levels where GIM (Glashow-Iliopolus-Maini) cancellations becomes very important. Also in most of the extensions of SM, loop graphs with new particles (most of the extensions of SM predict existence of some new particles like SUSY predicts whole set of SUSY particles) can contribute to the same order (in case of pure dileptonic decay of B_s meson SUSY can give a contribution which is many orders greater than SM contribution [1, 2]). In particular the process $B \rightarrow X_s \gamma$ and $B \rightarrow X_s \ell^+ \ell^-$ are experimentally very clean and can possibly be more sensitive to any new Physics beyond the SM. The new physics effects in the rare decays can come in two ways, one via the modifications of the existing (in SM) Wilson coefficients [3] and other via the introduction of some new operators (accompanied by new coefficients) [2, 4]. The inclusive decay mode ($B \rightarrow X_s \ell^+ \ell^-$) can be more sensitive than the radiative decay mode ($B \rightarrow X_s \gamma$) for testing any new physics model because in inclusive decay mode many more kinematical distributions like, lepton pair forward backward (FB) asymmetry, leptons polarization asymmetry etc. can be measured.

Various kinematical distributions of the inclusive mode have been studied in many earlier works [4, 5]. As also been proved in many of the works that lepton polarization asymmetry of final state leptons can give us useful information to fit parameters of SM and constraint new physics models [5, 6]. But recently it has been noted down, in case of inclusive decays by Bensalem et.al, [7] that one can in principle observe many more observables, like the double polarization asymmetries (polarization asymmetries when both the leptons are polarized), which

would be useful in further testing of the SM and probing physics beyond it. They inferred that even if we won't be able to tag b but can observe the final polarization state of both the leptons than also we can have more distributions than what we have if we would only be measuring the single lepton polarization asymmetries. But if we can also have *b-tagging* along with the measurement of the polarization of both the final state leptons, then many more kinematical distributions would be available to us, which could be useful in testing the structure of effective Hamiltonian and hence the physics underlying it. In our earlier work [8] we tried to estimate as to what would be the form of various double polarization distributions within SM for the exclusive mode $B \rightarrow K^* \tau^+ \tau^-$ and how these distributions gets modified by switching on the SUSY effects. This work is the extension of the work of Bensalem et.al., [7]. In their work they restricted themselves to SM operators. In this work we will extend the SM operator basis and will try to observe the aftereffects of this on the various double polarization asymmetries.

The quark level transition we would be interested in the present work is $b \rightarrow s \ell^+ \ell^-$. But as has been very well emphasized in literature that if we consider the Supersymmetric (SUSY) extension of the SM, than we have to extend the SM list of operators to include the operators arising from the exchange Neutral Higgs Bosons (NHBs) [1, 2, 4, 5, 9]. In case of pure-dileptonic decays of B-meson ($B_s \rightarrow \ell^+ \ell^-$) the NHBs can change the SM predictions by many orders of magnitude [1, 2, 9]. As the couplings of the NHBs to leptons is proportional to the lepton mass, hence these effects becomes more important if $\ell = \mu, \tau$. The SUSY extension of the SM predicts existence of two new operators, which were not present within SM. These new operators are responsible for the orders enhancement of the branching ratio of pure dileptonic decay mode of B-meson. In our analysis we will be going to consider these operators and will try to estimate the dependence of the various double polarization asymmetries on MSSM parameters.

The paper is organized as follows : In section II we will present the effective Hamiltonian we are considering. We will then write the matrix element for the quark

*Electronic address: naveen@physics.du.ac.in

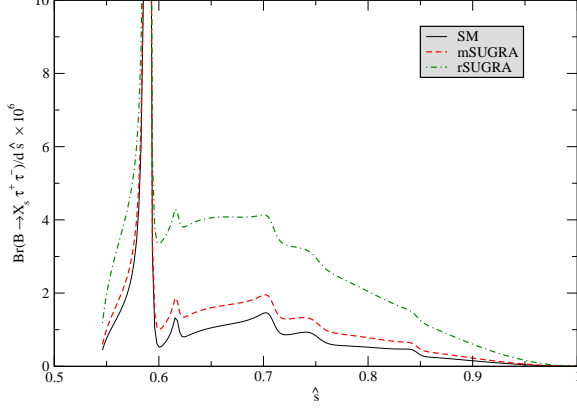


FIG. 1: Branching ratio of $B \rightarrow X_s \tau^+ \tau^-$ with scaled invariant mass of dileptons. Parameters of mSUGRA model are : $m = 400\text{GeV}$, $M = 500\text{GeV}$, $A = 0$, $\tan\beta = 40$ and $\text{sgn}(\mu)$ is positive. The additional parameter for rSUGRA is $m_A = 270\text{GeV}$

level process $b \rightarrow s \ell^+ \ell^-$. In section III we will give the definition and the analytical results of the double polarization asymmetries. Finally, we will conclude in section IV by discussing our numerical results.

II. EFFECTIVE HAMILTONIAN

We follow the convention followed in [4, 5] to write down the matrix element and invariant mass spectrum. The inclusive decay mode ($B \rightarrow X_s \ell^+ \ell^-$) is modeled by partonic process $b(p_b) \rightarrow s(p_s) + \ell^+(p_+) + \ell^-(p_-)$. This sort of modeling is actually the leading order calculation in $1/m_b$ expansion. By integrating out the heavy degrees of freedom from the full theory (MSSM here) we can get the effective Hamiltonian describing the semi-leptonic decay $b \rightarrow s \ell^+ \ell^-$ [1, 2, 4, 5] :

$$\mathcal{H}_{eff} = \frac{4G_F}{\sqrt{2}} V_{tb} V_{ts}^* \left(\sum_{i=1}^{10} C_i O_i + \sum_{i=1}^{10} C_{Q_i} Q_i \right) \quad (2.1)$$

where O_i are current-current ($i=1,2$), penguin ($i = 1, \dots, 6$), magnetic penguin ($i=7,8$) and semi-leptonic ($i = 9,10$) operators and C_i are the corresponding Wilsons. They have been given in [3, 10]. The additional operators Q_i ($i = 1, \dots, 10$) and their Wilson coefficients (C_{Q_i}) which arises due to MSSM diagrams are given in [1, 4].

Neglecting the mass of s-quark, the effective Hamiltonian gives the matrix element :

$$\mathcal{M} = \frac{\alpha G_F}{\sqrt{2}\pi} V_{tb} V_{ts}^* \left\{ \begin{aligned} & -2C_7^{eff} \frac{m_b}{q^2} (\bar{s} i \sigma_{\mu\nu} q^\nu P_R b) (\bar{\ell} \gamma^\mu \ell) \\ & + C_9^{eff} (\bar{s} \gamma_\mu P_L b) (\bar{\ell} \gamma^\mu \ell) + C_{10} (\bar{s} \gamma_\mu P_L b) (\bar{\ell} \gamma^\mu \gamma_5 \ell) \\ & + C_{Q_1} (\bar{s} P_R b) (\bar{\ell} \ell) + C_{Q_2} (\bar{s} P_R b) (\bar{\ell} \gamma_5 \ell) \end{aligned} \right\} \quad (2.2)$$

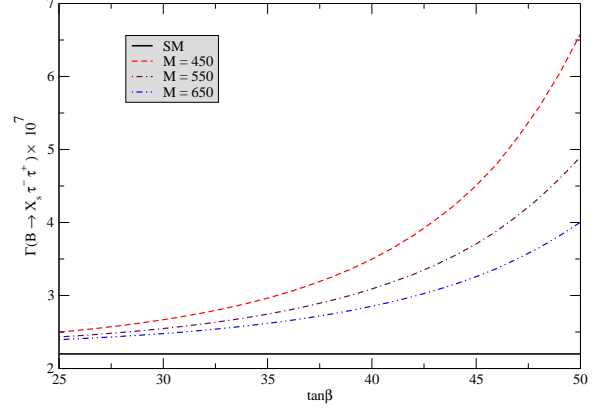


FIG. 2: Total decay rate with $\tan\beta$ in mSUGRA model. Other parameters $m = 400\text{GeV}$, $A = 0$

where q is the momentum transfer to the lepton pair given as $q = p_+ + p_-$, where p_- and p_+ are the momentas of ℓ^- and ℓ^+ respectively. $V_{tb} V_{ts}^*$ are the CKM factors and $P_{L,R} = (1 \mp \gamma_5)/2$.

The matrix element $\mathcal{M}(b \rightarrow s \ell^- \ell^+)$ is the free quark decay amplitude but it has some long distance effects also which comes due to the four-quark operators $\langle \ell^+ \ell^- s | O_i | b \rangle$ where $i = 1, \dots, 6$. These effects are absorbed into the redefinition of short distance Wilson coefficients according to the prescription given in many earlier works [6, 11]. The long distance effects are because of the $c\bar{c}$ resonance contributions. These resonances can be taken into account by using Breit-Wigner ansatz [6, 11] by which we add a term to C_9^{eff} . The resonance contribution to C_9^{eff} is :

$$C_9^{res} \propto \kappa \sum_{V=\psi} \frac{\hat{m}_V Br(V \rightarrow \ell^- \ell^+) \hat{\Gamma}_{total}^V}{\hat{s} - \hat{m}_V^2 + i \hat{m}_V \hat{\Gamma}_{total}^V} \quad (2.3)$$

where the symbols are explained in Kruger & Sehgal [6]. The phenomenological factor κ has to be introduced to reproduce the correct branching ratio $\mathcal{B}(B \rightarrow J/\Psi X_s) \rightarrow X_s \ell^+ \ell^-$. We will be going to take this factor to be 2.3 for our numerical analysis.

From the expression of the matrix element given in eqn.(2.2) we can get the dilepton invariant mass distribution as :

$$\frac{d\Gamma}{d\hat{s}} = \frac{G_F m_b^5}{192\pi^3} \frac{\alpha^2}{4\pi^2} |V_{tb} V_{ts}^*|^2 (1 - \hat{s})^2 \sqrt{1 - \frac{4\hat{m}_\ell^2}{\hat{s}}} \Delta \quad (2.4)$$

with

$$\begin{aligned} \Delta = & 4 \frac{(2 + \hat{s})}{\hat{s}} \left(1 + \frac{2\hat{m}_\ell^2}{\hat{s}} \right) |C_7^{eff}|^2 + (1 + 2\hat{s}) \\ & \left(1 + \frac{2\hat{m}_\ell^2}{\hat{s}} \right) |C_9^{eff}|^2 + (1 - 8\hat{m}_\ell^2 + 2\hat{s} + \frac{2\hat{m}_\ell^2}{\hat{s}}) \\ & \times |C_{10}|^2 + \frac{3}{2} (-4\hat{m}_\ell^2 + \hat{s}) |C_{Q_1}|^2 + \frac{3}{2} \hat{s} |C_{Q_2}|^2 \end{aligned}$$

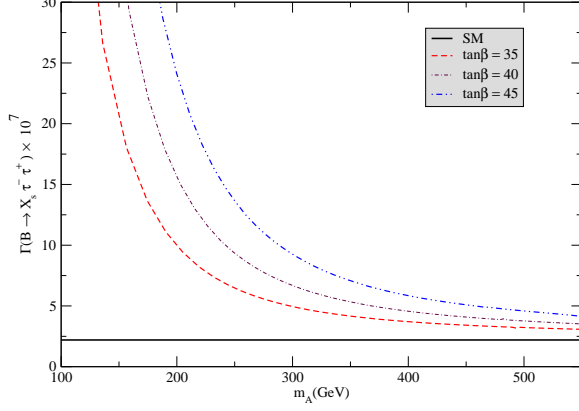


FIG. 3: Total decay rate with m_A GeV in rSUGRA model. Other parameters $m = 400$ GeV, $M = 500$ GeV, $A = 0$

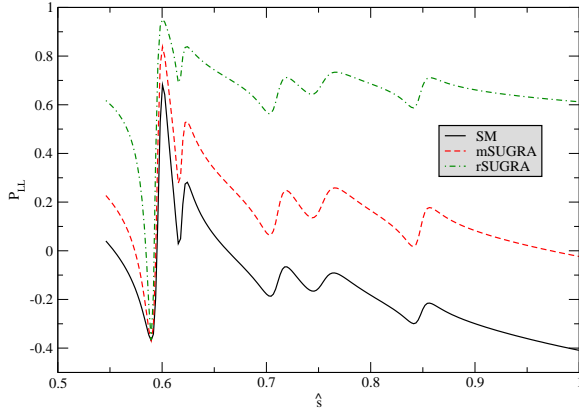


FIG. 4: \mathcal{P}_{LL} with \hat{s} with all the parameters same as in Fig. 1

$$\begin{aligned}
 &+12\left(1 + \frac{2\hat{m}_\ell^2}{\hat{s}}\right) \text{Re}(C_9^{eff*} C_7^{eff}) \\
 &+6\hat{m}_\ell \text{Re}(C_{10}^* C_{Q2}) \quad (2.5)
 \end{aligned}$$

Now ready with the expression of the invariant mass spectrum (including the scalar exchange effects) we will analyze various double polarization asymmetries in next section. As has been emphasized in many texts that the τ -polarization asymmetries in inclusive decay $B \rightarrow X_s \tau^+ \tau^-$ can be a very useful probe of the structure of effective Hamiltonian and hence the underlying theory. So for our analysis we will consider the inclusive decay channel with τ leptons in final state.

III. LEPTON POLARIZATION ASYMMETRIES

In this section we will evaluate the double lepton polarization asymmetries, i.e. where polarization of both the leptons is begin measured. For this we have to define the polarization vectors of ℓ^- and ℓ^+ . We will be going to use

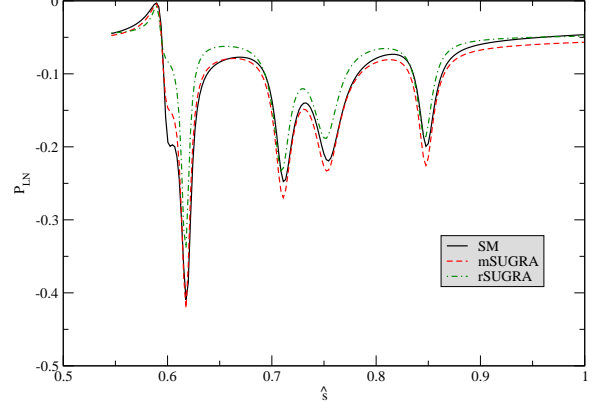


FIG. 5: \mathcal{P}_{LN} with \hat{s} with all the parameters same as in Fig.1

the convention as given in many earlier works [2, 4, 5]. To evaluate the polarized decay rates we have to introduce a spin projection operator defined by $N = 1/2(1 + \gamma_5 \mathcal{S}_x)$ for ℓ^- and $M = 1/2(1 + \gamma_5 \mathcal{W}_x)$ for ℓ^+ where $x = L, N, T$ and corresponds to the longitudinal, normal and transverse polarization asymmetries respectively. Firstly we define the orthogonal unit vectors S_x for ℓ^- and W_x for ℓ^+ in rest frames of ℓ^- and ℓ^+ respectively as :

$$\begin{aligned}
 S_L^\mu &\equiv (0, \mathbf{e}_L) = \left(0, \frac{\mathbf{p}_-}{|\mathbf{p}_-|}\right) \\
 S_N^\mu &\equiv (0, \mathbf{e}_N) = \left(0, \frac{\mathbf{p}_s \times \mathbf{p}_-}{|\mathbf{p}_s \times \mathbf{p}_-|}\right) \\
 S_T^\mu &\equiv (0, \mathbf{e}_T) = (0, \mathbf{e}_N \times \mathbf{e}_L) \quad (3.1)
 \end{aligned}$$

$$\begin{aligned}
 W_L^\mu &\equiv (0, \mathbf{w}_L) = \left(0, \frac{\mathbf{p}_+}{|\mathbf{p}_+|}\right) \\
 W_N^\mu &\equiv (0, \mathbf{w}_N) = \left(0, \frac{\mathbf{p}_s \times \mathbf{p}_+}{|\mathbf{p}_s \times \mathbf{p}_+|}\right) \\
 W_T^\mu &\equiv (0, \mathbf{w}_T) = (0, \mathbf{w}_N \times \mathbf{w}_L) \quad (3.2)
 \end{aligned}$$

where \mathbf{p}_- , \mathbf{p}_+ and \mathbf{p}_s are the three momentas of ℓ^- , ℓ^+ and strange (s) quark in center of mass frame (CM) frame of $\ell^- \ell^+$ respectively. Now from the rest frame of respective leptons we boost the four vectors S_x and W_x to the dilepton CM frame. Only the longitudinal vectors, S_L and W_L will get boosted by the Lorentz transformation to CM frame of $\ell^- \ell^+$ to a value :

$$\begin{aligned}
 S_L^\mu &= \left(\frac{|\mathbf{p}_-|}{m_\ell}, \frac{E_\ell \mathbf{p}_-}{m_\ell |\mathbf{p}_-|}\right) \\
 W_L^\mu &= \left(\frac{|\mathbf{p}_-|}{m_\ell}, -\frac{E_\ell \mathbf{p}_-}{m_\ell |\mathbf{p}_-|}\right) \quad (3.3)
 \end{aligned}$$

where E_ℓ is the energy of any of the leptons (both have same energy) in dileptonic CM frame.

Now we can define the double polarization asymmetries as [7] :

$$\mathcal{P}_{xy} \equiv \frac{\left(\frac{d\Gamma(S_x, W_y)}{d\hat{s}} - \frac{d\Gamma(-S_x, W_y)}{d\hat{s}}\right) - \left(\frac{d\Gamma(S_x, -W_y)}{d\hat{s}} - \frac{d\Gamma(-S_x, -W_y)}{d\hat{s}}\right)}{\left(\frac{d\Gamma(S_x, W_y)}{d\hat{s}} + \frac{d\Gamma(-S_x, W_y)}{d\hat{s}}\right) + \left(\frac{d\Gamma(S_x, -W_y)}{d\hat{s}} + \frac{d\Gamma(-S_x, -W_y)}{d\hat{s}}\right)} \quad (3.4)$$

where the sub-index x, y are L, N or T .

We can get the expressions of double polarization

asymmetries as :

$$\begin{aligned} \mathcal{P}_{LL} = & \frac{1}{\Delta} \left[-4 \frac{(2+\hat{s})}{\hat{s}} \left(1 - \frac{2\hat{m}_\ell^2}{\hat{s}}\right) |C_7^{eff}|^2 - (1+2\hat{s}) \left(1 - \frac{2\hat{m}_\ell^2}{\hat{s}}\right) |C_9^{eff}|^2 - (1-8\hat{m}_\ell^2+2\hat{s} - \frac{10\hat{m}_\ell^2}{\hat{s}}) |C_{10}|^2 \right. \\ & \left. + \frac{3}{2}(\hat{s}-4\hat{m}_\ell^2) |C_{Q_1}|^2 + \frac{3}{2}\hat{s} |C_{Q_2}|^2 - 12 \left(1 - \frac{2\hat{m}_\ell^2}{\hat{s}}\right) \text{Re}(C_7^{eff*} C_9^{eff}) + 6\hat{m}_\ell \text{Re}(C_{10}^* C_{Q_2}) \right] \end{aligned} \quad (3.5)$$

$$\begin{aligned} \mathcal{P}_{LN} = & \frac{3\pi}{2\sqrt{\hat{s}}\Delta} \left[2\hat{m}_\ell \text{Im}(C_{10}^* C_7^{eff}) - \hat{s} \text{Im}(C_7^{eff*} C_{Q_2}) + \hat{m}_\ell \text{Im}(C_{10}^* C_9^{eff}) - \frac{1}{2}\hat{s} \text{Im}(C_9^{eff*} C_{Q_2}) \right. \\ & \left. + \frac{1}{2}(\hat{s}-4\hat{m}_\ell^2) \text{Im}(C_{10}^* C_{Q_1}) \right] \end{aligned} \quad (3.6)$$

$$\begin{aligned} \mathcal{P}_{LT} = & \frac{3\pi}{2\sqrt{\hat{s}}\Delta} \sqrt{1 - \frac{4\hat{m}_\ell^2}{\hat{s}}} \left[-\hat{m}_\ell |C_{10}|^2 - 2\hat{m}_\ell \text{Re}(C_{10}^* C_7^{eff}) + \hat{s} \text{Re}(C_7^{eff*} C_{Q_1}) - \hat{m}_\ell \hat{s} \text{Re}(C_{10}^* C_9^{eff}) \right. \\ & \left. + \frac{1}{2}\hat{s} \text{Re}(C_9^{eff*} C_{Q_1}) - \frac{1}{2}\hat{s} \text{Re}(C_{10}^* C_{Q_2}) \right] \end{aligned} \quad (3.7)$$

$$\mathcal{P}_{NL} = -\mathcal{P}_{LN} \quad (3.8)$$

$$\begin{aligned} \mathcal{P}_{NN} = & \frac{1}{\Delta} \left[-4 \frac{(4\hat{m}_\ell^2 - \hat{s} + 2\hat{m}_\ell^2 \hat{s} + \hat{s}^2)}{\hat{s}^2} |C_7^{eff}|^2 + (-1 - 4\hat{m}_\ell^2 + \hat{s} - \frac{2\hat{m}_\ell^2}{\hat{s}}) (|C_9^{eff}|^2 + |C_{10}|^2) \right. \\ & \left. - \frac{3}{2}(\hat{s}-4\hat{m}_\ell^2) |C_{Q_1}|^2 + \frac{3}{2}\hat{s} |C_{Q_2}|^2 - 24 \frac{\hat{m}_\ell^2}{\hat{s}} \text{Re}(C_7^{eff*} C_9^{eff}) + 6 \frac{\hat{m}_\ell}{\hat{s}} \text{Re}(C_{10}^* C_{Q_2}) \right] \end{aligned} \quad (3.9)$$

$$\mathcal{P}_{NT} = \frac{2}{\Delta} \sqrt{1 - \frac{4\hat{m}_\ell^2}{\hat{s}}} \left[(1-\hat{s}) \text{Im}(C_{10}^* C_9^{eff}) + 3\hat{m}_\ell \text{Im}(C_{10}^* C_{Q_1}) - \frac{3}{2}\hat{s} \text{Im}(C_{Q_1}^* C_{Q_2}) \right] \quad (3.10)$$

$$\begin{aligned} \mathcal{P}_{TL} = & \frac{3\pi}{2\sqrt{\hat{s}}\Delta} \sqrt{1 - \frac{4\hat{m}_\ell^2}{\hat{s}}} \left[-\hat{m}_\ell |C_{10}|^2 + 2\hat{m}_\ell \text{Re}(C_{10}^* C_7^{eff}) - \hat{s} \text{Re}(C_7^{eff*} C_{Q_1}) + \hat{m}_\ell \hat{s} \text{Re}(C_{10}^* C_9^{eff}) \right. \\ & \left. - \frac{1}{2}\hat{s} \text{Re}(C_9^{eff*} C_{Q_1}) - \frac{1}{2}\hat{s} \text{Re}(C_{10}^* C_{Q_2}) \right] \end{aligned} \quad (3.11)$$

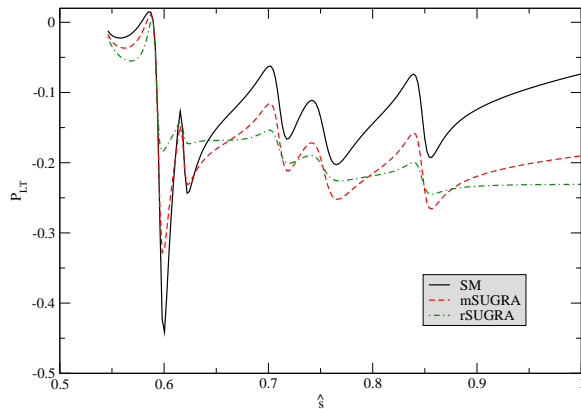
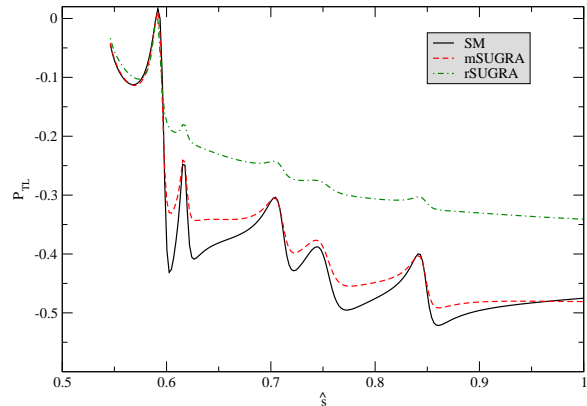
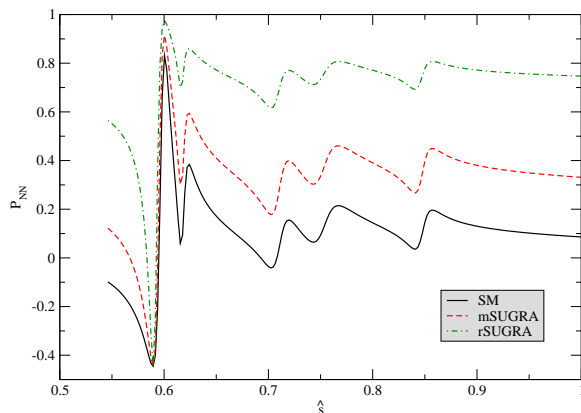
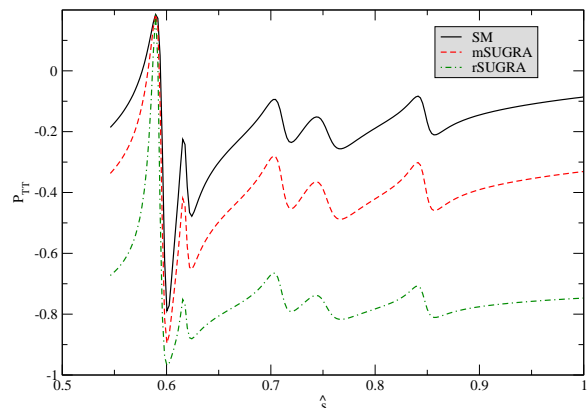
$$\mathcal{P}_{TN} = -\mathcal{P}_{NT} \quad (3.12)$$

$$\begin{aligned} \mathcal{P}_{TT} = & \frac{1}{\Delta} \left[-4 \frac{(-4\hat{m}_\ell^2 - \hat{s} - 2\hat{m}_\ell^2 \hat{s} + \hat{s}^2)}{\hat{s}^2} |C_7^{eff}|^2 + (-1 + 4\hat{m}_\ell^2 + \hat{s} + \frac{2\hat{m}_\ell^2}{\hat{s}}) |C_9^{eff}|^2 + (1 + 4\hat{m}_\ell^2 - \hat{s} - \frac{10\hat{m}_\ell^2}{\hat{s}}) |C_{10}|^2 \right. \\ & \left. + \frac{3}{2}(\hat{s}-4\hat{m}_\ell^2) |C_{Q_1}|^2 - \frac{3}{2}\hat{s} |C_{Q_2}|^2 + 24 \frac{\hat{m}_\ell^2}{\hat{s}} \text{Re}(C_7^{eff*} C_9^{eff}) - 6 \frac{\hat{m}_\ell}{\hat{s}} \text{Re}(C_{10}^* C_{Q_2}) \right] \end{aligned} \quad (3.13)$$

where Δ is given in eqn.(2.5).

IV. NUMERICAL ANALYSIS, RESULTS AND DISCUSSION

In this section we will be going to discuss our numerical analysis and the results of our numerical analysis. Firstly

FIG. 6: \mathcal{P}_{LT} with \hat{s} with all the parameters same as in Fig.1FIG. 8: \mathcal{P}_{TL} with \hat{s} with all the parameters same as in Fig.1FIG. 7: \mathcal{P}_{NN} with \hat{s} with all the parameters same as in Fig.1FIG. 9: \mathcal{P}_{TT} with \hat{s} with all the parameters same as in Fig.1

we will be going to list the SM values of the branching ratio of $B \rightarrow X_s \tau^+ \tau^-$ and various double polarization asymmetries we have presented in previous sections in Table I.

We have analyzed the SUSY effects on the various observables which we have listed in previous section. MSSM is although the simplest and the one having least number of parameters, extension of the SM. But still it has large number of parameters which makes it difficult to do phenomenology with it. But we do have some models, like Dilaton, moduli, mSUGRA, ...etc, which reduces this vast parameter space to a manageable level. In our numerical work we will be going to use one of the more popular unified model called Supergravity (SUGRA) model. The main feature of SUGRA (we will call this as minimal SUGRA or mSUGRA) model is that a unification of all the scalars, fermions and coupling constants is assumed at GUT scale. So effectively in mSUGRA framework we have five parameters which are : m (unified mass of all the scalars), M (unified mass of all the gauginos), A (universal trilinear coupling constant), $\tan\beta$ (ratio of vev of

the two Higgs doublets) and $sgn(\mu)$ ¹.

But as we know that universality of scalar masses at GUT scale is not a necessary condition of SUGRA [12]. One can in principle have a different unified mass of the squark sector and Higgs sector at GUT scale. We will explore this scenario also, which we will call as relaxed SUGRA (rSUGRA) model. The additional parameter which we will be going to have in this model we will take as mass of pseudo-scalar Higgs boson (m_A).

We will be going to work in the high $\tan\beta$ region of the SUGRA parameter space because its only in this region the effects of NHBs becomes more prominent. There are some constraints on the MSSM parameter space from experimental observations of $B \rightarrow X_s \gamma$ [13]. In our analysis we will be going to consider only that region of parameter

¹ the convention about $sgn(\mu)$ we will be going to follow is that it appears in chargino mass matrix with a +ve sign

$\text{Br}(B \rightarrow X_s \tau^+ \tau^-)$	\mathcal{P}_{LL}	\mathcal{P}_{LN}	\mathcal{P}_{LT}	\mathcal{P}_{NL}	\mathcal{P}_{NN}	\mathcal{P}_{NT}	\mathcal{P}_{TL}	\mathcal{P}_{TN}	\mathcal{P}_{TT}
1.29×10^{-7}	- 0.082	- 0.137	- 0.136	0.136	0.122	- 0.017	- 0.397	0.017	-0.216

TABLE I: Standard Model predictions of the observables for $B \rightarrow X_s \tau^+ \tau^-$

space which satisfy the 95% CL bound [13] :

$$2 \times 10^{-4} < \text{Br}(B \rightarrow X_s \gamma) < 4.5 \times 10^{-4}$$

which is agreement with CLEO and ALEPH results.

We will also present the numerical results of the average polarization asymmetries. The averaging procedure which we will be going to use is defined as :

$$\langle \mathcal{P} \rangle \equiv \frac{\int_{(3.646+0.02)^2/m_B^2}^{(m_B-m_{K^*})^2/m_B^2} \mathcal{P} \frac{d\Gamma}{d\hat{s}} d\hat{s}}{\int_{(3.646+0.02)^2/m_B^2}^{(m_B-m_{K^*})^2/m_B^2} \frac{d\Gamma}{d\hat{s}} d\hat{s}} \quad (4.1)$$

which means in integrating the observables we will be going to consider the region of dilepton invariant mass which is above the first charmonium resonance (after the threshold of the process $b \rightarrow s \tau^+ \tau^-$). We will be not going to present the result of \mathcal{P}_{NT} (and \mathcal{P}_{TN}) as they are very small.

We have presented the plots, of the various kinematical variables, we presented in sections II and III, with the (scaled) invariant mass of the dilepton. In Fig.1 we have shown the variation of the branching ratio of $B \rightarrow X_s \tau^+ \tau^-$ with dilepton invariant mass in three different models we have considered, namely SM, mSUGRA and rSUGRA. In Fig. 4, 5, 6, 7, 8 and 9 we have plotted the distributions of various double polarization asymmetries with dileptonic invariant mass. As we can see from these figures that SUSY can change these distributions substantially over the whole kinematically allowed region. We have done the detailed scanning of the mSUGRA and rSUGRA parameter space and have presented the results of the integrated polarization asymmetries, as defined in eqn.(4.1). In Fig. 10, 12, 14, 16, 18 and 20 we have shown the plots of various integrated polarization asymmetries with $\tan\beta$ for various values of M (the unified gaugino mass at GUT scale) in the mSUGRA model. As we can see that there is a substantial changes in the SM and mSUGRA model prediction. Specially for \mathcal{P}_{LL} where depending upon the mSUGRA parameters it can even change its sign. In Fig. 11, 13, 15, 17, 19 and 21 we have plotted various integrated polarization asymmetries as function m_A (mass of pseudo-scalar Higgs boson) for various values of $\tan\beta$. There also one can observe major changes in the predictions of various integrated polarization asymmetries as compared to SM values.

As has already been mentioned in many works [2, 5, 6, 7, 8] that polarization asymmetries are useful in finding out the structure of the effective Hamiltonian and hence the physics underlying it. As also been argued

by Bensalam et al. [7], if we work within the SM then for inclusive decay $B \rightarrow X_s \ell^+ \ell^-$ we have five theoretical parameters which are : four Wilsons (C_7, C_{10} , real and imaginary part of C_9^{eff}) and m_b , they can in principle be completely determined using the three τ^- polarization asymmetries, the total decay rate and the FB asymmetry i.e. five observables. But as known from earlier results [5, 6] the normal polarization asymmetry is very small and hence we have to consider the polarization asymmetry of τ^+ also. Also the measurement of FB asymmetry requires b-tagging. So if we have a untagged sample then the observables which we have are : decay rate, two polarization asymmetries of τ^- (we are neglecting the normal one being very small) and two polarization asymmetries of τ^+ (again neglecting the normal one). So we have five parameters and five observables which should in principle be sufficient. But there is no other constraint which will give us the cross-check of SM. So along these arguments Bensalam et.al. constructed double polarization asymmetries which give us large number of observables to have a good cross-checking of SM.

Let's now examine the situation if we believe in SUSY extension the SM. As has been argued in many works [1, 2, 4] that if we consider the decay channel $b \rightarrow s \tau^+ \tau^-$ in SUSY extension of SM², then we have to extend the SM list of operators by introduction of two new operators C_{Q_1} and C_{Q_2} . So now our theoretical parameters would be seven (five SM one and two new Wilson coefficients). So we require more number of observables to fix up this new structure of effective Hamiltonian and hence the double polarization asymmetries could possibly be very useful.

The model which we are considering is MSSM. In MSSM if we assume the MSSM parameters to be real then the only source of CP violation is the CKM matrix. The transition $b \rightarrow s \ell^+ \ell^-$ is a CP conserving process. Let's try to analyze the number of additional observables which we now have³. For this we consider two possibilities : one where we can have *b-tagging* and the other where there is no *b-tagging*. If we say that the double polarization asymmetries for $B \rightarrow X_s \tau^+ \tau^-$ are \mathcal{P}_{ij} then for the conjugated process $\bar{B} \rightarrow \bar{X}_s \tau^+ \tau^-$ we denote them with $\bar{\mathcal{P}}_{ij}$. But in general $\bar{\mathcal{P}}_{ij} = \pm \mathcal{P}_{ij}$ ⁴.

² in fact this is true even if we consider the two Higgs Doublet model (2HDM) extension of SM [9]

³ by additional observables we mean the observables due to measurement of double polarization asymmetries

⁴ in fact except for \mathcal{P}_{NL} and \mathcal{P}_{NT} the sign is always positive. For \mathcal{P}_{NL} and \mathcal{P}_{NT} the sign is negative

So if we consider the first case where there is no b -tagging. In a untagged sample we can measure four additional observables namely $\mathcal{P}_{LL}, \mathcal{P}_{NN}, \mathcal{P}_{TT}$ and $(\mathcal{P}_{LT} + \mathcal{P}_{TL})$.

But if we consider that we can tag b in that case we have all the nine double polarization asymmetries available to us which will give us very useful probes into the structure of effective Hamiltonian.

Acknowledgments

I am thankful to Prof. S. Rai Choudhury for useful discussions and comments during the course of the work. Thanks are due to Prof. D. London for initiation of this work which is the extension of his earlier work [7]. I am

also thankful to Dr. Ashok Goyal for carefully reading the manuscript. This work is supported under SERC scheme of Department of Science and Technology (DST), India.

APPENDIX A: INPUT PARAMETERS

$$\begin{aligned} m_B &= 5.26 \text{ GeV} , m_b = 4.8 \text{ GeV} , m_c = 1.4 \text{ GeV} \\ m_\tau &= 1.77 \text{ GeV} , m_w = 80.4 \text{ GeV} , \\ m_z &= 91.19 \text{ GeV} , V_{tb}V_{ts}^* = 0.0385 , \\ \alpha &= \frac{1}{129} , \Gamma_B = 4.22 \times 10^{-13} \text{ GeV} \\ G_F &= 1.17 \times 10^{-5} \text{ GeV}^{-2} \end{aligned}$$

-
- [1] S. R. Choudhury and N. Gaur, Phys. Lett. B **451**, 86 (1999), [arXiv:hep-ph/9810307] ; A. J. Buras, P. H. Chankowski, J. Rosiek and L. Slawianowska, Phys. Lett. B **546**, 96 (2002) [arXiv:hep-ph/0207241]; J. K. Mizukoshi, X. Tata and Y. Wang, Phys. Rev. D **66**, 115003 (2002) [arXiv:hep-ph/0208078]; T. Ibrahim and P. Nath, Phys. Rev. D **67**, 016005 (2003) [arXiv:hep-ph/0208142]; C. S. Huang and W. Liao, Phys. Lett. B **538**, 301 (2002) [arXiv:hep-ph/0201121]; S. Baek, P. Ko and W. Y. Song, Phys. Rev. Lett. **89**, 271801 (2002) [arXiv:hep-ph/0205259].
- [2] S. Baek, P. Ko and W. Y. Song, arXiv:hep-ph/0208112.
- [3] P. L. Cho, M. Misiak and D. Wyler, Phys. Rev. D **54**, 3329 (1996) [arXiv:hep-ph/9601360]; J. L. Hewett and J. D. Wells, Phys. Rev. D **55**, 5549 (1997) [arXiv:hep-ph/9610323].
- [4] Z. Xiong and J. M. Yang, Nucl. Phys. B **628**, 193 (2002)[arXiv:hep-ph/0105260] ; C. Bobeth, A. J. Buras, F. Kruger and J. Urban, Nucl. Phys. B **630**, 87 (2002) [arXiv:hep-ph/0112305] ; C. Huang, W. Liao and Q. Yan, Phys. Rev. D **59**, 011701 (1999), [arXiv:hep-ph/9803460].
- [5] S. Rai Choudhury, A. Gupta and N. Gaur, Phys. Rev. D **60**, 115004 (1999)[arXiv:hep-ph/9902355] ; S. Fukae, C. S. Kim and T. Yoshikawa, Phys. Rev. D **61**, 074015 (2000)[arXiv:hep-ph/9908229] ; D. Guetta and E. Nardi, Phys. Rev. D **58**, 012001 (1998) [arXiv:hep-ph/9707371].
- [6] F. Krüger and L. M. Sehgal, Phys. Lett. B **380**, 199 (1996), [arXiv:hep-ph/9603237] ; J. L. Hewett, Phys. Rev. D **53**, 4964 (1996), [arXiv:hep-ph/9506289].
- [7] W. Bensalem, D. London, N. Sinha and R. Sinha, Phys. Rev. D **67**, 034007 (2003) [arXiv:hep-ph/0209228].
- [8] S. Rai Choudhury, N. Gaur, A. S. Cornell and G. C. Joshi hep-ph/0304084.
- [9] W. Skiba and J. Kalinowski, Nucl. Phys. B **404**, 3 (1993) ; H. E. Logan and U. Nierste, Nucl. Phys. B **586**, 39 (2000), [arXiv:hep-ph/0004139] ; Y. Dai, C. Huang and H. Huang, Phys. Lett. B **390**, 257 (1997), [arXiv:hep-ph/9607389] .
- [10] B. Grinstein, M. J. Savage and M. B. Wise, Nucl. Phys. B **319**, 271 (1989) ; A. J. Buras and M. Münz, Phys. Rev. D **52**, 186 (1995) [arXiv:hep-ph/9501281].
- [11] A. Ali, T. Mannel and T. Morozumi, Phys. Lett. B **273**, 505 (1991); C. S. Lim, T. Morozumi and A. I. Sanda, Phys. Lett. B **218**, 343 (1989); N. G. Deshpande, J. Trampetic and K. Panose, Phys. Rev. D **39**, 1461 (1989); P. J. O'Donnell and H. K. Tung, Phys. Rev. D **43**, 2067 (1991) .
- [12] T. Goto, Y. Okada, Y. Shimizu and M. Tanaka, Phys. Rev. D **55**, 4273 (1997) [arXiv:hep-ph/9609512] ; T. Goto, Y. Okada and Y. Shimizu, Phys. Rev. D **58**, 094006 (1998) [arXiv:hep-ph/9804294] ; J. R. Ellis, K. A. Olive and Y. Santoso, arXiv : hep-ph/0204192.
- [13] B Physics at Tevatron : Run II & Beyond , K. Anikeev *et. al.* arXiv : hep-ph/0201071 ; CLEO collaboration, T.E.Coan *et. al.* Phys. Rev. Lett. **84**, 5283 (2000) [arXiv:hep-ex/9908022] ; ALEPH Collaboration, R.Barate *et. al.* Phys. Lett. B **429**, 169 (1998) .

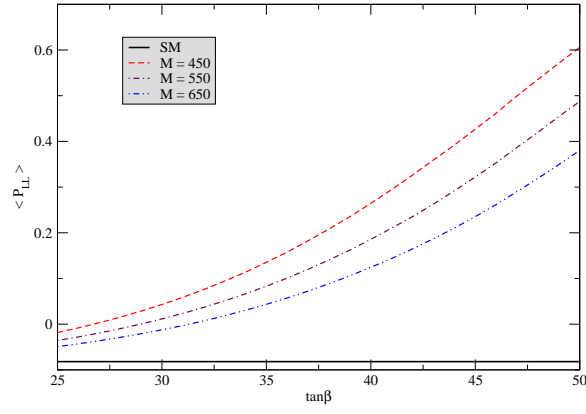


FIG. 10: Integrated \mathcal{P}_{LL} with $\tan\beta$ in mSUGRA model. Parameters same as given in Fig.2

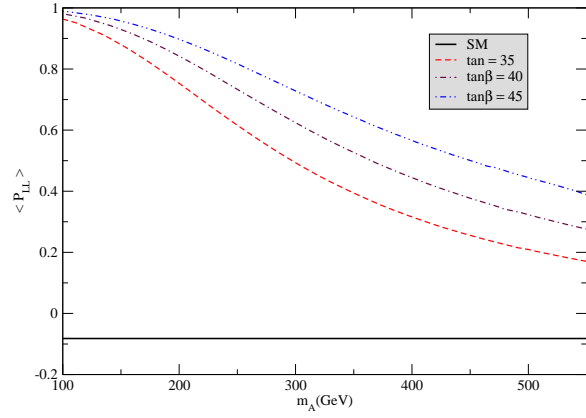


FIG. 11: Integrated \mathcal{P}_{LL} with m_A GeV in rSUGRA model. Parameters same as given in Fig. 3

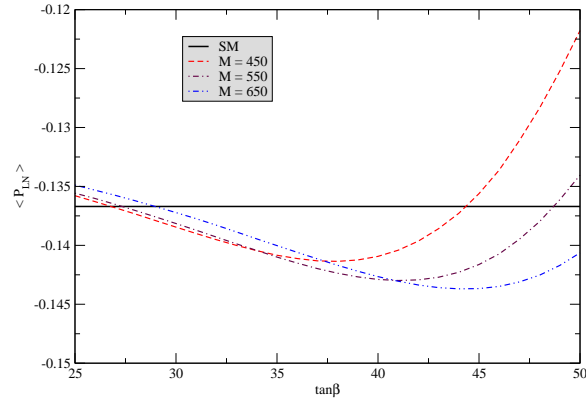


FIG. 12: Integrated \mathcal{P}_{LN} with $\tan\beta$ in mSUGRA model. Parameters same as given in Fig.2

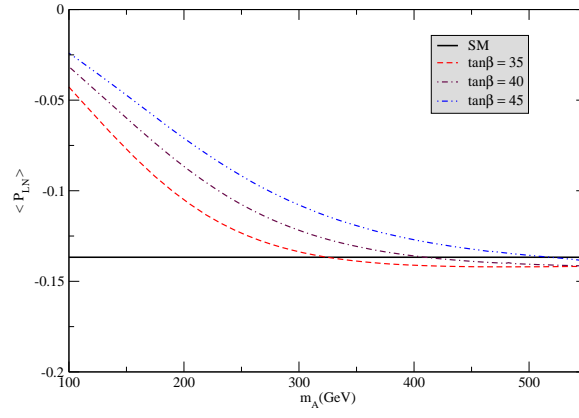


FIG. 13: Integrated \mathcal{P}_{LN} with m_A GeV in rSUGRA model. Parameters same as given in Fig.3

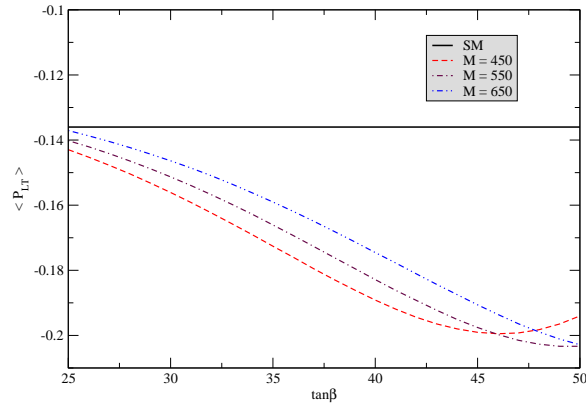


FIG. 14: Integrated \mathcal{P}_{LT} with $\tan\beta$ in mSUGRA model. Parameters same as given in Fig. 2

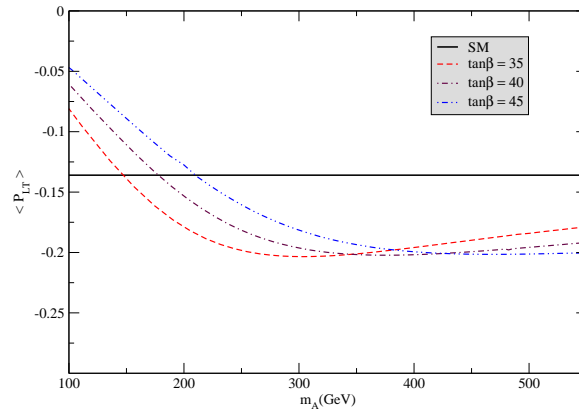


FIG. 15: Integrated \mathcal{P}_{LT} with m_A GeV in rSUGRA model. Parameters same as given in Fig. 3

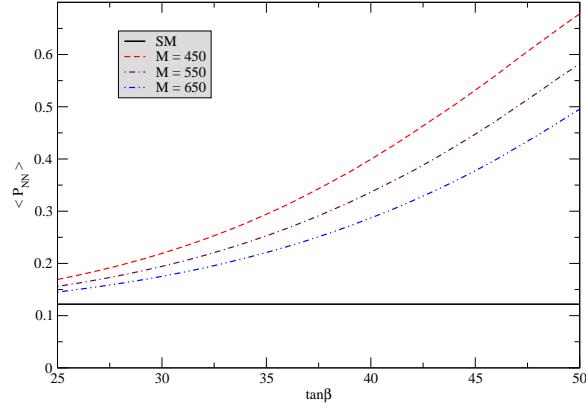


FIG. 16: Integrated \mathcal{P}_{NN} with $\tan\beta$ in mSUGRA model. Parameters same as given in Fig. 2

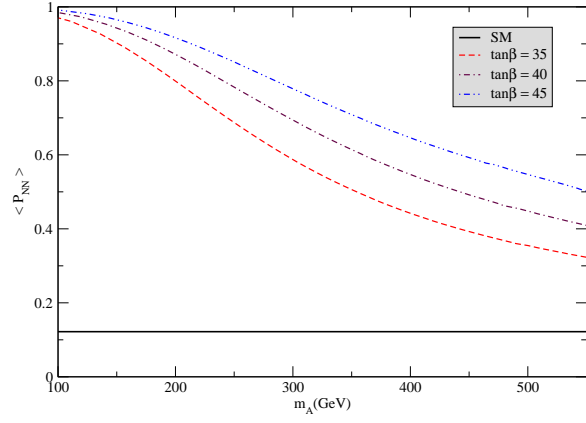


FIG. 17: Integrated \mathcal{P}_{NN} with m_A GeV in rSUGRA model. Parameters same as given in Fig. 3

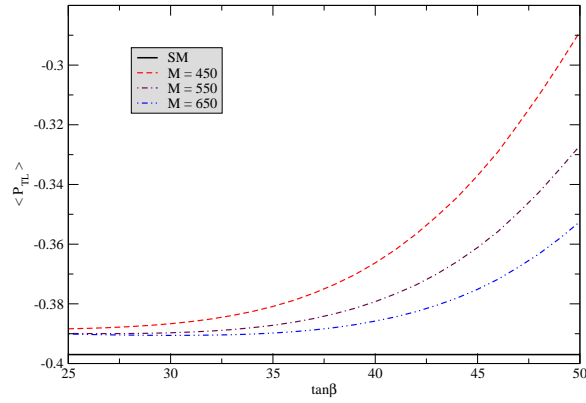


FIG. 18: Integrated \mathcal{P}_{TL} with $\tan\beta$ in mSUGRA model. Parameters same as given in Fig. 2

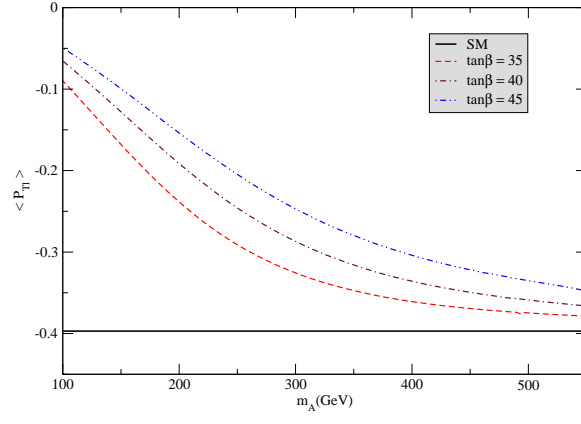


FIG. 19: Integrated \mathcal{P}_{TL} with m_A GeV in rSUGRA model. Parameters same as given in Fig. 3

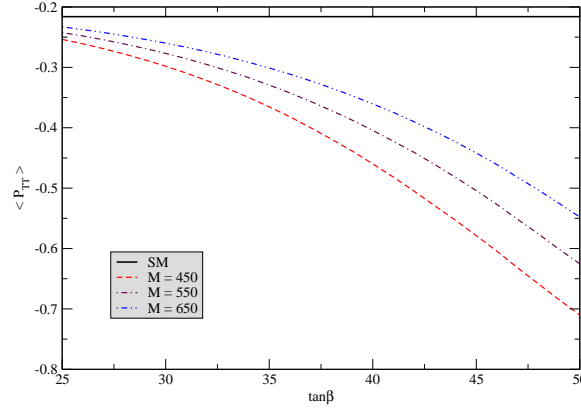


FIG. 20: Integrated \mathcal{P}_{TT} with $\tan\beta$ in mSUGRA model. Parameters same as given in Fig. 2

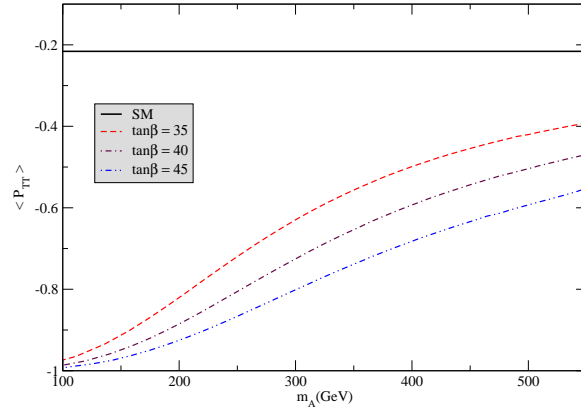


FIG. 21: Integrated \mathcal{P}_{TT} with m_A GeV in rSUGRA model. Parameters same as given in Fig. 3